



Universiteit
Leiden
The Netherlands

The role of ATF2 in insulin action

Baan, B.

Citation

Baan, B. (2009, June 23). *The role of ATF2 in insulin action*. Retrieved from <https://hdl.handle.net/1887/13861>

Version: Corrected Publisher's Version

License: [Licence agreement concerning inclusion of doctoral thesis in the Institutional Repository of the University of Leiden](#)

Downloaded from: <https://hdl.handle.net/1887/13861>

Note: To cite this publication please use the final published version (if applicable).

6

Increased *in vivo* phosphorylation of ATF2 by insulin and high fat diet-induced insulin resistance in mice

Manuscript in preparation

Chapter 6

Chapter 6

Increased *in vivo* phosphorylation of ATF2 by insulin and high fat diet-induced insulin resistance in mice

Bart Baan¹, Peter J. Voshol², Gerard C.M. van der Zon¹, Jan Kriek¹,
 Elena Korshennikova¹, Johannes A. Romijn², J. Antonie Maassen^{1,3}
 and D. Margriet Ouwens¹

¹Departments of Molecular Cell Biology, and ²Endocrinology, Leiden University Medical Centre, Leiden, The Netherlands, and ³Department of Endocrinology/Diabetes Centre, VU University Medical Centre, Amsterdam, the Netherlands

Activating transcription factor 2 (ATF2) has been identified as a component of insulin signalling in cultured cells. ATF2-activation has been linked to the regulation of metabolic enzymes, but also to β -cell apoptosis, inflammation and diabetic neuropathy. To detail the function of ATF2 in insulin action, we studied the induction of ATF2-phosphorylation and potential ATF2 target genes by insulin *in vivo* and examined the effects of high-fat diet (HFD) induced insulin resistance on these parameters in mice. Insulin infusion induced a transient increase in ATF2-phosphorylation in the liver, white adipose tissue (WAT) and pancreas. In the liver, insulin infusion increased the expression of the potential ATF2-target genes ATF3, *c-jun*, *Egr1*, and SREBP1c. In the absence of insulin, basal ATF2 phosphorylation was increased in the liver and WAT of HFD-fed mice. This was accompanied by increased hepatic mRNA levels of the pro-inflammatory cytokines IL1 β and TNF α , in addition to ATF3, *c-jun*, *Egr1*, and SREBP1c. Furthermore, the livers from HFD-fed mice were resistant for the induction of ATF2-target genes by insulin. We conclude that ATF2 has a dual role in insulin action as it is activated both by insulin infusion and under conditions of HFD-induced insulin resistance. The induction of pro-inflammatory cytokines in the liver of HFD-fed mice only suggests a state of chronic inflammation, which may contribute to the development of type 2 diabetes.

Activating transcription factor 2 (ATF2) is a component of the insulin signaling system. In A14 fibroblasts and 3T3L1 adipocytes, insulin rapidly phosphorylates ATF2 on its transactivation sites, Thr69 and Thr71 (1;2). This phosphorylation results in activation of the protein and induction of ATF2-target genes, including ATF3, *c-jun*, *Egr1*, MKP1 and SREBP1c (3). Also other studies indicate a role for ATF2 in metabolic control. In skeletal muscle and brown adipose tissue, the p38/ATF2 pathway regulates the expression of PPAR γ coactivator 1 α (PGC1 α) (4;5), and of phosphoenolpyruvate carboxykinase (PEPCK) in the hepatoma cells (6;7). Finally, studies on the *Drosophila* fat body, the equivalent of the mammalian liver and adipose tissue, identify the p38/ATF2/PEPCK pathway as critical regulator of lipid metabolism (8).

It should be noted, however, that several ATF2-target genes are also highly linked to the pathogenesis of insulin resistance, β -cell dysfunction and complications found in type 2 diabetes. In β -cells, the ATF2-mediated induction of both the pro-inflammatory cytokine interleukin 1 β (IL1 β) and ATF3, in response to nitric oxide, hyperglycemia, high levels of palmitate, pro-inflammatory cytokines or endoplasmic reticulum stress, precedes apoptosis

Chapter 6

(9-11). In endothelial cells, Egr1-regulated genes, like platelet-derived growth factor, TNF α , intracellular adhesion molecule-1, monocyte chemoattractant protein-1, plasminogen activator inhibitor-1, and vascular adhesion molecule-1, have been implicated in the development of atherosclerosis (12;13). Finally, uncontrolled activation of SREBP1c has been implicated in the development of hepatic steatosis, which aggravates insulin resistance (14;15). Interestingly, also the upstream regulator of ATF2, JNK, has been linked to the pathogenesis of insulin resistance. Hirosumi et al. found elevated JNK activity in liver, adipose tissue and skeletal muscle of obese insulin resistant mice, and knockout of *Jnk1* (*Jnk1*^{-/-}) or inhibition of JNK-activity restores insulin sensitivity in mouse models of insulin resistance (16;17). It has been proposed that JNK phosphorylates the insulin receptor substrate 1 on Ser307, thereby inhibiting the insulin-mediated activation of protein kinase B, a master regulator of glucose metabolism (18;19).

The elevated basal activity of JNK, and the involvement of, amongst others, ATF3, IL1 β , Egr1, and SREBP1c in β -cell apoptosis and insulin resistance, suggests that deregulation of ATF2 activity may contribute to the pathogenesis of type 2 diabetes mellitus. The present study aimed at detailing the role of ATF2 in insulin action and insulin resistance. Therefore, we analyzed the *in vivo* phosphorylation of ATF2 and the expression of ATF2-target in insulin target tissues of mice before and after an insulin infusion. Furthermore, we examined whether these responses were altered under conditions of high-fat diet-induced insulin resistance and obesity.

Results

Insulin induces ATF2 phosphorylation in vivo. We used male C57/B16J mice, fasted overnight, to examine ATF2 phosphorylation following an infusion with either PBS or insulin. To ascribe alterations in ATF2 phosphorylation levels to insulin rather than changes in blood glucose levels, glucose was co-infused to maintain euglycemia. Table 1 lists the animal characteristics at sacrifice. Mean body weight was similar among the experimental groups. Plasma insulin levels were 77 \pm 10 pmol/L in PBS-infused mice and 435 \pm 96 pmol/L and 467 \pm 84 pmol/L following 10 and 20 min of insulin infusion (both P <0.01 versus PBS). Blood glucose levels were similar in all groups (Table 1).

Table 1. Characteristics of overnight fasted mice following PBS or insulin infusion

	PBS (n=7)	10 min INS (n=6)	20 min INS (n=7)
Body weight at sacrifice (gram)	24.2 \pm 0.6	23.6 \pm 0.7	22.9 \pm 0.7
Fasting blood glucose (mmol/L)	6.2 \pm 0.7	5.6 \pm 0.6	6.4 \pm 0.7
Glucose at sacrifice (mmol/L)	5.7 \pm 0.4	4.7 \pm 0.4	4.8 \pm 0.4
Insulin at sacrifice (pmol/L)	77 \pm 17	435 \pm 96*	467 \pm 84*

Values are mean \pm SEM, *, P <0.05 versus PBS

Immunohistochemical staining (IHC) with phospho-ATF2-Thr71 antibodies shows a nuclear staining throughout the liver and pancreas of insulin-infused mice only (Figure 1). Notably, in the pancreas, ATF2-Thr71 phosphorylation tended to be enriched in the insulin-secreting β -cells (Figure 1). Application of the phospho-ATF2-Thr69+71 antibody failed to produce a detectable signal in IHC (data not shown).

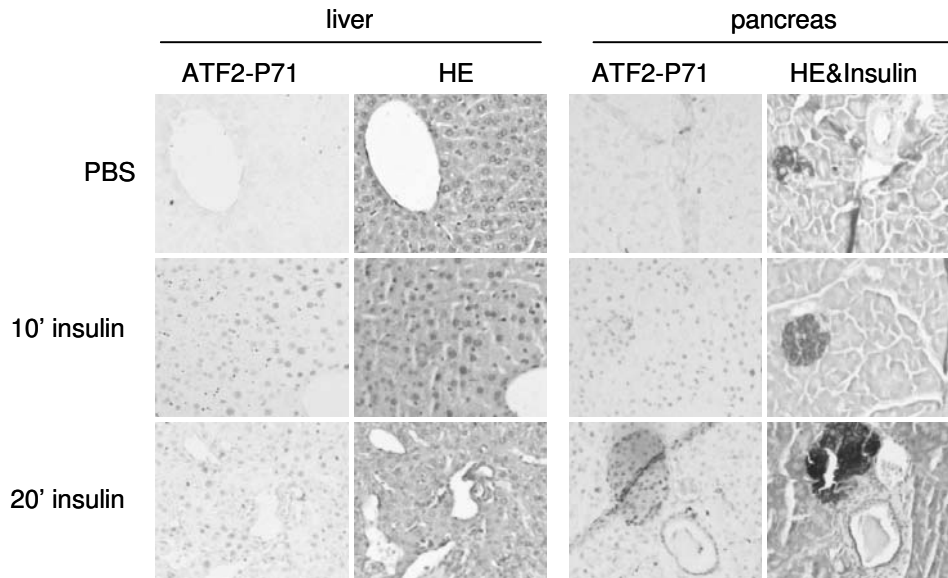


Figure 1. Immunohistochemical staining of mouse liver and pancreas tissue sections with phospho-ATF2-Thr71 antibodies (ATF2-P71), or hematoxylin (HE; blue) in combination with insulin (brown). Mice were infused with either PBS or insulin for the indicated times. Photographs are representative of 2-3 independent animals. Full-colour illustration can be found at page 127.

Instead, we examined the insulin-mediated induction of ATF2-Thr71 and ATF2-Thr69+71 phosphorylation in homogenates of insulin target tissues. Ten minutes after initiation of the insulin infusion, ATF2-Thr71 phosphorylation levels were increased 2.9-fold in liver ($P < 0.05$ versus PBS-infusion, Figure 2). At this time point, phosphorylation levels of ATF2-Thr69+71 were increased 2.6-fold ($P < 0.05$ versus PBS infusion, Figure 2). Hepatic ATF2 was still phosphorylated after 20 min insulin infusion (Figure 2), but had returned to basal levels 2 hrs after insulin infusion (data not shown).

In epididymal adipose tissue, all phospho-ATF2 antibodies detected a band migrating at ~64-kDa rather than the 70-kDa band observed in the liver. This protein was also detected by an antibody recognizing the aminoterminal part of ATF2 and was downregulated upon silencing the ATF2 gene in murine fibroblasts (data not shown). Therefore, it is likely that the observed immunoreactivity in adipose tissue results from an alternative splice variant of ATF2 (Chapter 2). The immunoreactivity of phospho-ATF2-Thr71 was increased by 2.3- and 2.5-fold after 10 and 20 min of insulin infusion, respectively ($P < 0.05$; Figure 2). In contrast to the liver, ATF2-Thr69+71 phosphorylation was not significantly affected by insulin in adipose tissue (Figure 2).

Because of the multiple cell types present in the pancreas, we used cultured rat INS-1E insulinoma cells to confirm insulin-mediated ATF2 phosphorylation in insulin-secreting β -cells. Insulin rapidly increased both ATF2-Thr71- and ATF2-Thr69+71-phosphorylation, with peak levels occurring at 5 min after insulin addition, followed by a gradual decrease after 15 and 30 min (Figure 2). The increases in ATF2 phosphorylation by western blot could not be ascribed to major changes in ATF2 protein levels (Figure 2).

Chapter 6

In heart and skeletal muscle, we could not detect the induction of ATF2 phosphorylation following insulin infusion, despite the presence of ATF2 protein in these tissues (data not shown). Activation of insulin signalling in all tissues was confirmed by increased phosphorylation of the PKB/Akt substrate PRAS40 (20) in insulin-infused animals (Figure 2, data not shown).

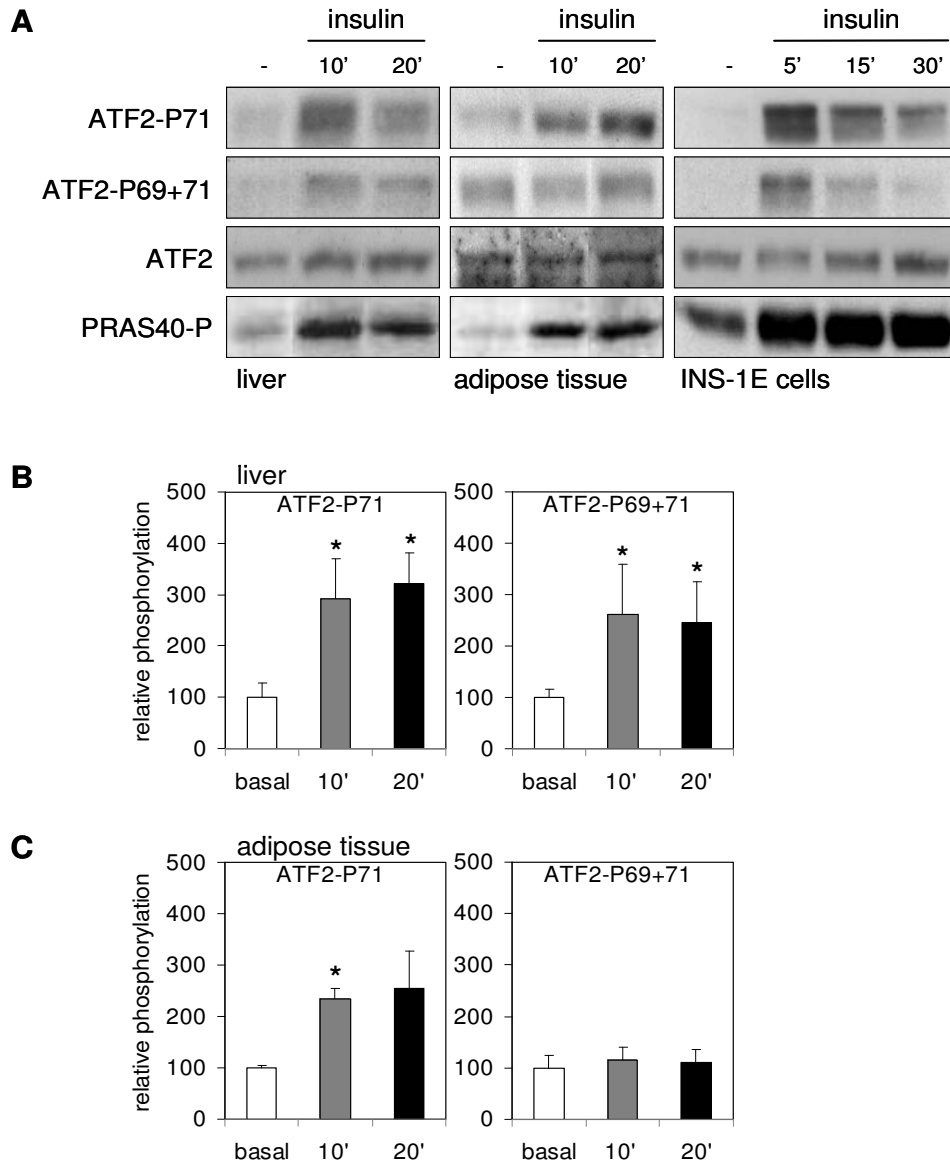


Figure 2. A. Phosphorylation of ATF2 and PRAS40, and expression of ATF2 in mouse liver and adipose tissue homogenates following infusion with PBS or insulin, and INS-1E cells, following incubation with 1 μ M insulin for the indicated amounts of time. Western blots are representative of 7 independent mice per group or 2 independent experiments and verified for equal loading by PonceauS staining (not shown). B/C. Quantification of ATF2 phosphorylation in the liver (B) and adipose tissue (C). The relative ATF2 phosphorylation after PBS infusion (basal) was set at 100. Data are expressed as mean \pm SEM of 7 independent mice per group. *, $P < 0.05$ versus basal.

ATF2-phosphorylation *in vivo*

Induction of ATF2-target genes by insulin. Using real-time PCR, we examined the expression of 10 potential ATF2-target genes, i.e. ATF3, *c-jun*, Egr1, HIF1 α , IL1 β , MKP1, PEPCK, PGC1 α , SREBP1c, TNF α in mouse livers. Livers were isolated from chow-fed mice, after an overnight fast or 2 h after initiation of a hyperinsulinemic euglycemic clamp. Table 2 shows that the mean body weight was similar between the experimental groups. Plasma insulin levels were 136 \pm 18 pmol/L in PBS-infused mice and 454 \pm 108 pmol/L following 2 h hyperinsulinemia. Blood glucose levels were similar between the groups (Table 2).

As shown in Figure 3, hyperinsulinemia increased the expression of ATF3, *c-jun*, Egr1 and SREBP1c by 1.4-, 1.4-, 2.7- and 3.0 fold (all $P < 0.05$ vs basal), respectively. Furthermore, insulin lowered the levels of 4 genes (HIF1 α , PEPCK, PGC1 α and TNF α) and did not affect the abundance of IL1 β and MKP1 (Figure 3).

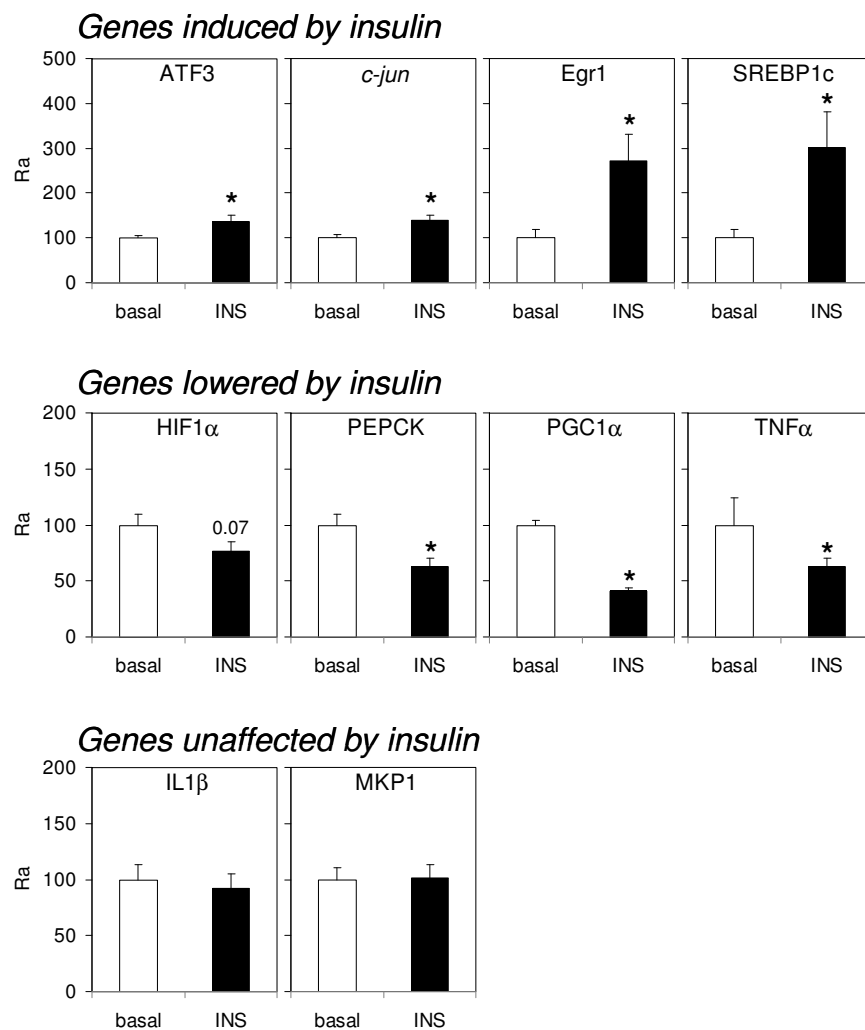


Figure 3. Effect of hyperinsulinemia on the expression of ATF2-target genes. Mice, fasted overnight, were sacrificed before (basal; open bars) or 2 h after initiation of a hyperinsulinemic euglycemic clamp (INS; black bars). Gene expression levels in the liver were determined by real-time PCR. The relative mRNA abundance (Ra) in the liver from fasted mice was set at 100. Data are expressed as mean \pm SEM. *, $P < 0.05$ versus basal ($n = 6-8$ mice/group).

Chapter 6

Table 2. Body and plasma characteristics before and after initiation of a hyperinsulinemic euglycemic clamp in mice fed a chow or HFD for 6 weeks.

	basal		hyperinsulinemia	
	chow (n=7)	HFD (n=7)	Chow (n=5)	HFD (n=6)
Body weight at sacrifice (gram)	24.3±0.6	28.1±1.0*	26.1±1.1	30.6±1.3*
Fasting blood glucose (mmol/L)	4.2±0.4	4.2±0.2	4.6±0.5	4.4±0.2
Fasting plasma insulin (pmol/L)	136±18	190±42*	139±25	185±31*
Glucose at sacrifice (mmol/L)	4.2±0.4	4.2±0.2	4.4±0.2	4.2±0.2
Insulin at sacrifice (pmol/L)	136±18	190±42*	454±108	592±188

Values are mean±SEM, *, $P<0.05$ versus chow

Insulin resistance increases basal ATF2 phosphorylation in mice. The effects of insulin resistance on ATF2-phosphorylation were determined in tissues from high-fat diet (HFD) fed mice (21). Table 2 shows that compared to chow fed mice, a 6-wk exposure to a HFD induced obesity. Whereas fasting blood glucose levels were not affected by high-fat feeding, fasting plasma insulin levels were elevated in HFD-fed mice. We previously reported that HFD-feeding blunted the suppression of hepatic glucose production by insulin (21), indicating insulin resistance.

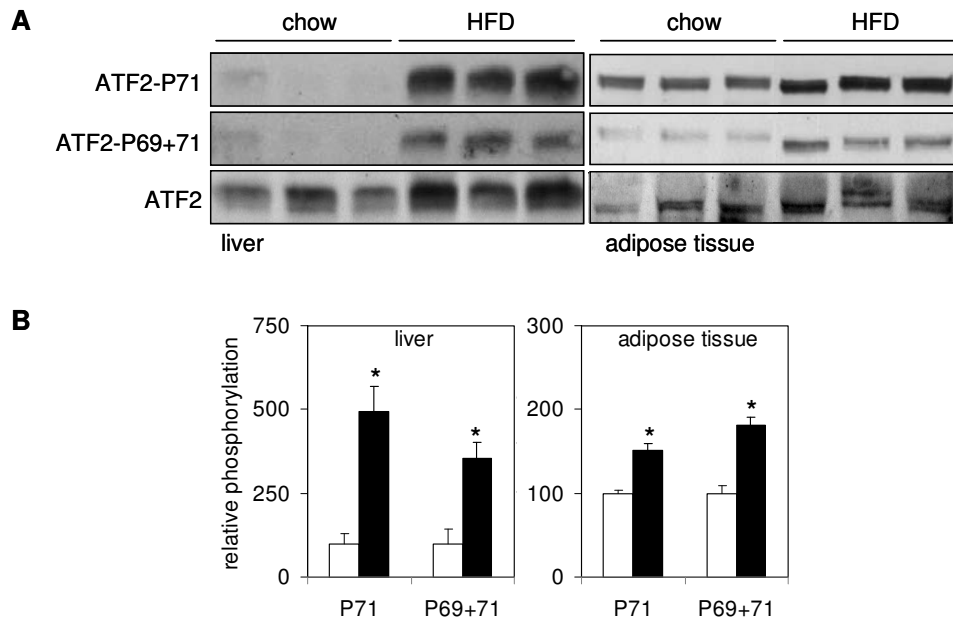


Figure 4. Western blot (A) and quantification (B) ATF2 phosphorylation in the liver and adipose tissue of chow (open bars) or high-fat diet fed mice (black bars). Tissue homogenates of were analyzed by immunoblotting with antibodies recognizing total ATF2, phospho-ATF2-Thr71 (ATF2-P71) or phospho-ATF2-Thr69+71 (ATF2-P69+71) antibodies. PonceauS staining confirmed equal loading of the Western blots (not shown). The relative ATF2 phosphorylation in chow fed mice was set at 100. Data are expressed as mean±SEM of 4 independent mice per group. *, $P<0.05$ versus chow.

In the liver, HFD-feeding induced a 4.9- and 3.6-fold increase in ATF2-Thr71 and ATF2-Thr69+71 phosphorylation, respectively (Figure 4; $P<0.005$ and $P<0.01$ respectively). Also in epididymal adipose tissue, phosphorylation levels of ATF2-Thr71 and ATF2-Thr69+71 were increased in HFD-fed mice by 1.5- ($P<0.001$) and 1.8-fold ($P<0.005$), respectively (Figure 4). This increase in basal levels of phosphorylated ATF2 could not be ascribed to alterations in ATF2 protein expression (Figure 4).

Increased mRNA levels of ATF2-target genes in the liver of HFD-fed mice. We also determined whether the elevated levels of phosphorylated ATF2 in livers from HFD-fed mice were accompanied by alterations in the expression of potential ATF2-target genes. Figure 5A shows that the abundance of ATF3, *c-jun*, Egr1, IL1 β , SREBP1c and TNF α was 1.7-, 1.8-, 4.0-, 1.7-, 12.8- and 2.1-fold higher, respectively, in livers from HFD- versus CH-fed mice (all $P<0.05$).

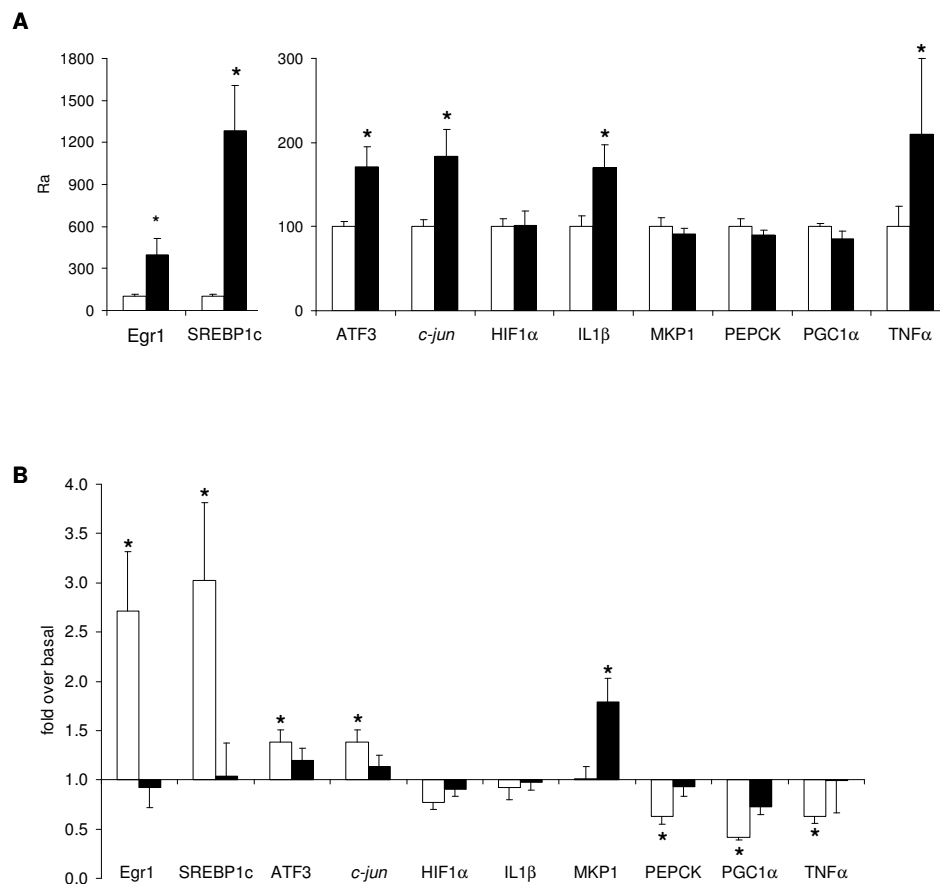


Figure 5. Effect of high-fat feeding on the expression of ATF2-target genes. A. Gene expression levels determined by real-time PCR in livers, isolated after an overnight fast, from mice fed a chow (open bars) or a high-fat diet (black bars). The relative mRNA abundance (Ra) in the liver from chow-fed mice was set at 100. Data are expressed as mean \pm SEM. *, $P<0.05$ versus basal ($n=6-8$ mice/group). B. Effect of 2h hyperinsulinemia on the expression of ATF2 target genes in chow (open bars) and high-fat diet (black bars) fed mice. The effect of insulin is expressed as fold over basal. Data are mean \pm SEM. *, $P<0.05$ versus basal ($n=6-8$ mice/group).

Chapter 6

HFD-feeding had no effect on the expression of HIF1 α , MKP1, PEPCK and PGC1 α mRNA (Figure 5A). Except for MKP1, hyperinsulinemia did not significantly alter the expression of the examined genes, indicating that HFD-induced insulin resistance also affects insulin regulation of the ATF2 signaling pathway (Figure 5B).

Discussion

In this study, we examined the effects of insulin and HFD-feeding on the phosphorylation of the transcription factor ATF2. We show that insulin infusion induced phosphorylation of ATF2 on Thr69 and Thr71 in the liver, epididymal adipose tissue and the pancreas, but not in cardiac and skeletal muscle. In the liver, insulin increased the expression of the ATF2-regulated genes ATF3, *c-jun*, Egr1 and SREBP1c. Compared to chow-fed mice, HFD-feeding increased ATF2 phosphorylation in liver and adipose tissue. Elevated mRNA-levels of the (putative) ATF2-target genes ATF3, *c-jun*, Egr-1, SREBP1c, but also of the pro-inflammatory cytokines IL1 β and TNF α accompanied these HFD-induced changes in the liver. Finally, livers from HFD-fed mice were resistant for the induction of ATF2-target genes in response to insulin.

The present study extends our previous findings (1;2) and identifies ATF2 as a component of physiological insulin action *in vivo*. The study described here was performed with insulin concentrations normally achieved following food intake and under euglycemic conditions, thereby excluding the possibility that the observed phosphorylation of ATF2 results from alterations in plasma glucose levels.

Strikingly, in the fasted state with low plasma concentrations of insulin, the levels of phosphorylated ATF2 were markedly increased in both the liver and epididymal adipose tissue from insulin resistant HFD-fed mice. This indicates a role for ATF2 both in insulin action and insulin resistance. The predominant kinases regulating ATF2 phosphorylation are ERK1/2, p38 and JNK (1;2;22-25). Numerous studies have demonstrated elevated activity of predominantly JNK under conditions of insulin resistance (16;17;19;26;27). Therefore, the sustained ATF2 phosphorylation in tissues from HFD-fed animals is likely to result from elevated JNK-activity.

To detail the dual function of ATF2 in insulin action and insulin resistance, the expression levels of potential downstream targets of ATF2 were determined in the livers from CH- and HFD-fed mice. Four genes that have been linked with ATF2-activation in previous reports, i.e. HIF1 α (28), PEPCK (6-8), PGC1 α (4;5) and MKP1 (28;29), were neither induced by hyperinsulinemia in CH-fed mice nor by HFD-feeding. Tissue-specific differences in the expression of ATF2 isoforms which affect the composition of ATF2-containing heterodimers may contribute to the absence of ATF2-regulation of these genes. Furthermore, also other insulin- or HFD-induced signaling pathways may be dominant over the ATF2-pathway. For example, the PKB/FOXO pathway, which is strongly activated by insulin, has been shown to lower the expression of PEPCK (30) and PGC1 α (31).

Intriguingly, both HFD-feeding and hyperinsulinemia in CH-fed mice increased the abundance of 4 potential ATF2-regulated transcription factors, i.e. ATF3, *c-jun*, Egr1 and SREBP1c mRNA (3;22;28;32). It should be noted, however, that the magnitude of the induction caused by HFD-feeding, in particular of Egr1 and SREBP1c and to a lesser extent ATF3 and *c-jun*, is much higher than that caused by hyperinsulinemia in CH-fed mice. Furthermore, IL1 β and TNF α mRNA levels were increased in the livers of HFD-fed mice only.

It is unknown whether these changes can be ascribed to the duration of ATF2 phosphorylation, which is transient in response to insulin and continuous after HFD-feeding, or to changes in the composition of ATF2-containing dimers. In this respect, it should be noted that cJun is not only an important dimer partner of ATF2 (33), but that it is also phosphorylated by JNK (22;23). Thus, increases in both the phosphorylation and expression of c-jun may affect the activity and formation of cJun/ATF2 heterodimers in HFD-fed mice.

The identification of ATF3, like ATF2, a member of the ATF/CREB family of transcription factors (34), as insulin-regulated gene is surprising. Although ATF3 has been implicated in the downregulation of PEPCK (35), induction of ATF3 is strongly linked to inducers of (endoplasmic reticulum) stress and apoptosis. Elevated levels of ATF3 in β -cells, caused by exposure to hyperglycemia, IL1 β or nitric oxide (36), induce apoptosis via repression of the IRS2 gene (37). Furthermore, ATF3 is linked to mitochondrial dysfunction in C2C12 cells and negatively regulates the expression of adiponectin in 3T3L1 adipocytes (38;39).

Egr1 is linked to the regulation of cell proliferation and differentiation, amongst others by the induction of the homeodomain transcription factor pancreas duodenum homeobox-1 (PDX1), a key regulator of insulin expression and pancreatic β -cell development, function and survival (40). Also insulin signalling itself is critical for β -cell proliferation (41). Thus, an impaired induction of Egr1 by insulin may result in a decreased ability of the pancreas to compensate for the increased demand for insulin secretion under conditions of insulin resistance. Deregulation of Egr1 activity has further been linked to the development of atherosclerosis through enhanced expression of Egr1-target genes in endothelial cells (12;13) and adipocytes (42;43).

SREBP1c is a pivotal regulator of glucose and lipid metabolism, amongst others by inducing the expression of glucokinase and genes involved in lipogenesis (14;44). Both insulin and HFD-feeding are known inducers of SREBP1c in various tissues (45;46). However, unregulated activation of SREBP1c in the liver leads to hepatic steatosis, which aggravates insulin resistance (16).

The pathogenesis of type 2 diabetes is closely associated with chronic inflammation as illustrated by abnormal pro-inflammatory cytokine production by various tissues (47). The selective increases in IL1 β and TNF α in the livers of HFD-fed mice only support these findings. These pro-inflammatory cytokines are not only target of ATF2, but also potent inducers of ATF2 activation. A limitation of this study is that we could not determine the plasma levels of IL1 β and TNF α . However, it seems plausible that increases in circulating levels of pro-inflammatory cytokines may underlie the increased phosphorylation of ATF2 in the liver and WAT of HFD-fed mice, as has been observed by others (27;47).

Although the use of animal models can provide valuable information on deregulation of ATF2 under conditions of insulin resistance when compared to cultured cell lines, a major limitation is that we cannot formally ascribe the observed changes in gene expression to increases in ATF2 phosphorylation. Furthermore, we cannot exclude that the increased expression of IL1 β and TNF α in HFD-fed mice results from Kupffer cells or infiltrated macrophages (27;47). To resolve these issues, studies on mice with tissue-specific ablation of the ATF2 gene are required.

We conclude that we have identified ATF2 as a component of the insulin signalling system in the liver, pancreas and WAT. However, we also show that ATF2-

Chapter 6

activity is elevated in the liver and WAT of HFD-fed mice, which may contribute to the development of type 2 diabetes. This dual role of ATF2 suggests that regulation of ATF2 activity plays a critical role in insulin action and insulin resistance.

Materials and methods

Animals. The investigation conformed to the Guide for the Care and Use of Laboratory Animals as published by the NIH (NIH Publication No. 85-23, revised 1996) and the regulations of the Institutional Animal Care and Use Committee.

The effects of insulin infusion on ATF2-phosphorylation were studied in adult male C57Bl6J mice. Overnight fasted mice were anaesthetized by intraperitoneal injection with a combination of 6.25 mg/kg body weight (BW) acetylpromazine (Sanofi Santé Nutrition Animale, Libourne Cedex, France), 6.25 mg/kg BW midazolam (Roche, Mijdrecht, Netherlands) and 0.3125 mg/kg BW fentanyl (Janssen-Cilag, Tilburg, Netherlands). Insulin was infused through the tail-vein at 24.5 pmol/kg BW/min as described (48). Glucose was co-infused with insulin at 105 μ mol/min to maintain euglycemia. At 10 and 20 min following initiation of the insulin infusion, mice were sacrificed by cervical dislocation. Control animals were sacrificed following infusion with PBS. After sacrifice, organs were removed and either immersion-fixed in 4% buffered formaldehyde solution, or snap-frozen in liquid nitrogen and stored at -80°C until further use. The effects of insulin resistance were examined in high-fat diet fat mice. Male C57Bl6/J mice were randomly divided in two groups and fed either standard lab chow or a high-fat diet (HFD). After 6 weeks on the diet, mice were sacrificed following infusion with PBS or 2-hrs after initiation of a hyperinsulinemic euglycemic clamp (insulin infusion rate: 24.5 pmol/kg BW/min) as described (21). Then, tissues were removed, snap-frozen in liquid nitrogen and stored at -80°C until further use.

Diets. High-fat diet was obtained from Arie Blok Diervoeding (Woerden, The Netherlands, cat#4031.05) and consisted (in % of total energy) of 44% bovine fat, 19% protein and 37% carbohydrate. Chow diet consisted of 32% proteins, 54% carbohydrates and 14% crude fat. Both diets were supplemented with vitamins and microelements.

Plasma determinations. Blood glucose was measured using a FreeStyle hand glucometer (Therasense, Disetronic Medical Systems, Vianen, Netherlands). Plasma insulin levels were determined using ELISA (Ultrasensitive mouse insulin kit, Mercodia AB, Uppsala, Sweden).

Cell culture. Ins-1E insulinoma cells (49) were kindly provided by Dr. C. Wollheim (University Medical Center, Geneva, Switzerland) and cultured in RPMI 1640 supplemented with 9% fetal bovine serum (FBS), 25 mM HEPES, glutamax, 1 mM sodium pyruvate and antibiotics.

Immunohistochemistry. Fixed tissues were prepared by routine paraffin embedding, sections were cut and mounted on slides. Sections were deparaffinized and washed with water for 5 min. Antigen retrieval was performed for ATF2 by boiling in 10 mM citrate buffer at pH 6 for 10 min followed by cooling for 20 min. Sections were washed three times for 5 minutes with water and endogenous peroxidase activity was blocked in 1% H_2O_2 for 20 min. After washing in water and PBS, sections were preincubated with 5% normal goat serum in PBS for 1 h. Incubation with ATF2-phospho-Thr71 antibodies (#9221; Cell Signaling Technology, Beverly, MA, USA) (1:50) was overnight at 4°C (50). Sections were then washed with PBS, incubated with rabbit Envision-HRP for 30 min, washed again and developed using DAB with 0.7% NiCl_2 for 10 min (black/blue precipitate). Separate sections were counterstained with hematoxylin (blue) or in case of the

ATF2-phosphorylation *in vivo*

pancreas with insulin (brown) and hematoxylin (blue) (51). Therefore, sections were incubated with 1% H₂O₂, washed and incubated overnight with the insulin-antibody (Dako, Glostrup, Denmark) (1:200) at room temperature, followed by washing with PBS, incubation with rabbit Envision-HRP for 30 min, washing and developing using DAB for 10 min. Sections were inspected using a Leica DM-LB light microscope (Leica, Rijswijk, The Netherlands) and digital images were captured using a Leica DC500 digital camera and software.

Western blotting. Cell- and tissue homogenates were prepared in 30 mM Tris.Cl, pH 7.5, 150 mM NaCl, 0.5% Triton X-100, 0.5% sodium deoxycholate, 1% SDS, 1 mM Na₃VO₄, 10 mM NaF and protease inhibitors (Complete, Roche) and cleared by centrifugation (13.200 rpm; 15 min, 4°C). Protein content was determined using a BCA protein assay kit (Pierce, Rockford, IL, USA). Expression and phosphorylation of proteins was determined by SDS-PAGE and immunoblotting (2). The antibodies used were: anti-phospho-Thr71-ATF2 (#9221), anti-phospho-Thr69+71-ATF2 (#9225) (both from Cell Signaling Technology, Beverly, MA, USA), anti-ATF2 (C19) (Santa Cruz Biotechnology, Inc., Santa Cruz, CA, USA) and anti-phospho-PRAS40-Thr246 (#44-100G) (Biosource International, Camarillo, CA, USA). PonceauS staining of the membranes confirmed correct protein transfer and equal loading. Bound antibodies were visualized by enhanced chemiluminescence. Immunoblots were quantified by densitometric analysis of the films (52).

RNA extraction and real-time PCR analysis. Frozen tissue biopsies (~30 mg) were homogenized in RLT-buffer (Qiagen, Venlo, The Netherlands), whereafter total RNA was extracted using RNeasy mini columns (Qiagen, Venlo, The Netherlands). DNase I digestion was performed to ensure complete removal of DNA. Purity and quantity of nucleic acids was determined by spectrophotometric analysis at 260 and 280 nm. Integrity of the RNA was verified by agarose gel electrophoresis. A total of 1.0 µg RNA was transcribed into complementary DNA using a Superscript™ first strand synthesis kit (Invitrogen, Breda, The Netherlands) using oligo-dT priming. mRNA abundance was measured using real-time PCR. Primers are listed in Table 3 and were designed using Primer Express version 3.0 software (Applied Biosystems, Foster City, CA, USA). Reactions were carried out in the presence of 1x SYBR® Green PCR Master Mix (Applied Biosystems), 0.5µM of each forward and reverse primer on a ABI PRISM® 7900HT Sequence Detection System (Applied Biosystems) with the following cycle conditions: 95°C for 10 min followed by 40 cycles of 95°C for 15", 60°C for 30" and 72°C for 30". The threshold cycle number (C_t) was calculated using SDS software version 2.2 (Applied Biosystems) and an automated setting of the baseline. Data were analyzed using a comparative critical threshold (C_t) method in which the amount of target is normalized to the amount of endogenous control using the equation $R_a = 2^{-\Delta C_t}$ in which R_a = the relative mRNA abundance and $\Delta C_t = C_t(\text{gene of interest}) - C_t(\text{endogenous control})$ and $C_t(\text{endogenous control})$ is calculated as the geomean(C_t) of β-actin and EF1α. The expression of these genes was not affected by the experimental conditions used in this study.

Statistical analysis. Data are expressed as means ± SE. Differences between groups were determined by unpaired students two-tailed *t*-test using SPSS version 16.0. *P*<0.05 was considered statistically significant.

Chapter 6

Table 3. Sequences of primers used for real-time PCR

Gene name	Accession number	Forward primer (5'→3')	Reverse primer (5'→3')
ATF2	NM_001025093	gactccaacgccaacaagat	aggtaaagggtgtcctggt
ATF3	NM_007498	aacacctctgccatc	ttatttctttctcgccgcctc
β-actin	NM_007393	agagggaaatcgtgctgac	caatagtgatgacctggccgt
c-jun	NM_010591	caacatgctcagggaaacaggt	tgcgttagcatgagttggca
EF1α	NM_010106	aattggaggcattggcac	aaaggtaaccaccatgccagg
Egr1	NM_007913	aacactttgtggcctgaacc	aggcagaggaagacgatgaa
IL1β	NM_008361	caggcaggcagtatcactca	aggtgctcatgtcctcatcc
MKP1	NM_013642	ctcatgggagctggtcctta	gcgaagaaactgcctcaaac
PEPCK	NM_011044	tctgaggccacagctgctg	gggtcgcgatggcaaagg
PGC1α	NM_008904	tttttggtgaaattgaggaatgc	cggtaggtgatgaaacatagct
SREBP1c	NM_011480	ggagccatggattgcacatt	cctgtctcacccccagcata
TNFα	NM_013693	gtcccaaagggatgagaag	cacttggtggtttgctacga

Acknowledgements

The authors acknowledge Dr. Claes Wollheim (University Medical Center, Geneva, Switzerland) for the kind gift of INS-1E cells and the contribution of Annemieke van der Wal (Leiden University Medical Center, Dept. of Pathology) and Dr. Ng Hang Le (Leiden University Medical Center, Dept. of Human Genetics) to the immunohistochemistry experiments. The support of the Dutch Diabetes Research Foundation (grants 2001.00.046, 2002.00.032 and 2005.01.003) and the European Science Foundation (COST-Action BM0602) is greatly acknowledged. P.J.V. is the recipient of a VIDI-Innovational Research Grant from the Netherlands Organization for Health Research and Development.

References

1. Ouwens, D. M., de Ruiter, N. D., van der Zon, G. C., Carter, A. P., Schouten, J., van der Burgt, C., Kooistra, K., Bos, J. L., Maassen, J. A., and van Dam H. (2002) *EMBO J.* **21**, 3782-3793
2. Baan, B., van Dam H., van der Zon, G. C., Maassen, J. A., and Ouwens, D. M. (2006) *Mol. Endocrinol.* **20**, 1786-1795
3. Baan et al., *Manuscript in preparation* (Chapter 5)
4. Yan, Z., Li, P., and Akimoto, T. (2007) *Exerc. Sport Sci. Rev.* **35**, 97-101
5. Cao, W., Daniel, K. W., Robidoux, J., Puigserver, P., Medvedev, A. V., Bai, X., Floering, L. M., Spiegelman, B. M., and Collins, S. (2004) *Mol. Cell Biol.* **24**, 3057-3067
6. Cheong, J., Coligan, J. E., and Shuman, J. D. (1998) *J. Biol. Chem.* **273**, 22714-22718
7. Lee, M. Y., Jung, C. H., Lee, K., Choi, Y. H., Hong, S., and Cheong, J. (2002) *Diabetes* **51**, 3400-3407
8. Okamura, T., Shimizu, H., Nagao, T., Ueda, R., and Ishii, S. (2007) *Mol. Biol. Cell.* **18**, 1519-1529
9. Ammendrup, A., Maillard, A., Nielsen, K., Aabenhus, A. N., Serup, P., Dragsbaek, M. O., Mandrup-Poulsen, T., and Bonny, C. (2000) *Diabetes.* **49**, 1468-1476

10. Zhang, S., Liu, H., Liu, J., Tse, C. A., Dragunow, M., and Cooper, G. J. (2006) *FEBS J.* **273**, 3779-3791
11. Reimold, A. M., Kim, J., Finberg, R., and Glimcher, L. H. (2001) *Int. Immunol.* **13**, 241-248
12. Wang, C. C., Sharma, G., and Draznin, B. (2006) *Am. J. Hypertens.* **19**, 366-372
13. Hasan, R. N., Phukan, S., and Harada, S. (2003) *Arterioscler. Thromb. Vasc. Biol.* **23**, 988-993
14. Ferre, P. and Foufelle, F. (2007) *Horm. Res.* **68**, 72-82
15. Shimomura, I., Matsuda, M., Hammer, R. E., Bashmakov, Y., Brown, M. S., and Goldstein, J. L. (2000) *Mol. Cell* **6**, 77-86
16. Hirosumi, J., Tuncman, G., Chang, L., Gorgun, C. Z., Uysal, K. T., Maeda, K., Karin, M., and Hotamisligil, G. S. (2002) *Nature* **420**, 333-336
17. Stebbins, J. L., De, S. K., Machleidt, T., Becattini, B., Vazquez, J., Kuntzen, C., Chen, L. H., Cellitti, J. F., Riel-Mehan, M., Emdadi, A., Solinas, G., Karin, M., and Pellecchia, M. (2008) *Proc. Natl. Acad. Sci. U. S. A* **105**, 16809-16813
18. de Luca C. and Olefsky, J. M. (2008) *FEBS Lett.* **582**, 97-105
19. Hotamisligil, G. S. (2005) *Diabetes.* **54 Suppl 2:S73-8.**, S73-S78
20. Nascimento, E. B., Fodor, M., van der Zon, G. C., Jazet, I. M., Meinders, A. E., Voshol, P. J., Vlasblom, R., Baan, B., Eckel, J., Maassen, J. A., Diamant, M., and Ouwens, D. M. (2006) *Diabetes.* **55**, 3221-3228
21. Korshennikova, E., van der Zon, G. C., Voshol, P. J., Janssen, G. M., Havekes, L. M., Grefhorst, A., Kuipers, F., Reijngoud, D. J., Romijn, J. A., Ouwens, D. M., and Maassen, J. A. (2006) *Diabetologia.* **49**, 3049-3057
22. van Dam, H., Wilhelm, D., Herr, I., Steffen, A., Herrlich, P., and Angel, P. (1995) *EMBO J.* **14**, 1798-1811
23. Gupta, S., Campbell, D., Derijard, B., and Davis, R. J. (1995) *Science.* **267**, 389-393
24. Raingeaud, J., Gupta, S., Rogers, J. S., Dickens, M., Han, J., Ulevitch, R. J., and Davis, R. J. (1995) *J. Biol. Chem.* **270**, 7420-7426
25. Kyriakis, J. M. and Avruch, J. (2001) *Physiol Rev.* **81**, 807-869
26. Solinas, G., Naugler, W., Galimi, F., Lee, M. S., and Karin, M. (2006) *Proc. Natl. Acad. Sci. U. S. A.* **103**, 16454-16459
27. Wellen, K. E. and Hotamisligil, G. S. (2005) *J. Clin. Invest* **115**, 1111-1119
28. Hayakawa, J., Mittal, S., Wang, Y., Korkmaz, K. S., Adamson, E., English, C., Ohmichi, M., McClelland, M., and Mercola, D. (2004) *Mol. Cell.* **16**, 521-535
29. Breitwieser, W., Lyons, S., Flenniken, A. M., Ashton, G., Bruder, G., Willington, M., Lacaud, G., Kouskoff, V., and Jones, N. (2007) *Genes Dev.* **21**, 2069-2082
30. Barthel, A. and Schmoll, D. (2003) *Am. J. Physiol Endocrinol. Metab* **285**, E685-E692
31. Daitoku, H., Yamagata, K., Matsuzaki, H., Hatta, M., and Fukamizu, A. (2003) *Diabetes* **52**, 642-649
32. Liang, G., Wolfgang, C. D., Chen, B. P., Chen, T. H., and Hai, T. (1996) *J. Biol. Chem.* **271**, 1695-1701
33. Benbrook, D. M. and Jones, N. C. (1990) *Oncogene* **5**, 295-302
34. Hai, T. W., Liu, F., Coukos, W. J., and Green, M. R. (1989) *Genes Dev.* **3**, 2083-2090
35. Allen-Jennings, A. E., Hartman, M. G., Kociba, G. J., and Hai, T. (2002) *J. Biol. Chem.* **277**, 20020-20025
36. Hartman, M. G., Lu, D., Kim, M. L., Kociba, G. J., Shukri, T., Buteau, J., Wang, X., Frankel, W. L., Guttridge, D., Prentki, M., Grey, S. T., Ron, D., and Hai, T. (2004) *Mol. Cell Biol.* **24**, 5721-5732

Chapter 6

37. Li, D., Yin, X., Zmuda, E. J., Wolford, C. C., Dong, X., White, M. F., and Hai, T. (2008) *Diabetes* **57**, 635-644
38. Kim, H. B., Kong, M., Kim, T. M., Suh, Y. H., Kim, W. H., Lim, J. H., Song, J. H., and Jung, M. H. (2006) *Diabetes*. **55**, 1342-1352
39. Lim, J. H., Lee, J. I., Suh, Y. H., Kim, W., Song, J. H., and Jung, M. H. (2006) *Diabetologia*. **49**, 1924-1936
40. Eto, K., Kaur, V., and Thomas, M. K. (2007) *J. Biol. Chem.* **282**, 5973-5983
41. Leibiger, I. B. and Berggren, P. O. (2008) *Annu. Rev. Nutr.* **28**, 233-251
42. Alexander-Bridges, M., Buggs, C., Giere, L., Denaro, M., Kahn, B., White, M., Sukhatme, V., and Nasrin, N. (1992) *Mol. Cell Biochem.* **109**, 99-105
43. Sartipy, P. and Loskutoff, D. J. (2003) *J. Biol. Chem.* **278**, 52298-52306
44. Eberle, D., Hegarty, B., Bossard, P., Ferre, P., and Foufelle, F. (2004) *Biochimie* **86**, 839-848
45. Raghov, R., Yellaturu, C., Deng, X., Park, E. A., and Elam, M. B. (2008) *Trends Endocrinol. Metab* **19**, 65-73
46. Lin, J., Yang, R., Tarr, P. T., Wu, P. H., Handschin, C., Li, S., Yang, W., Pei, L., Uldry, M., Tontonoz, P., Newgard, C. B., and Spiegelman, B. M. (2005) *Cell* **120**, 261-273
47. Hotamisligil, G. S. (2006) *Nature* **444**, 860-867
48. Voshol, P. J., Haemmerle, G., Ouwens, D. M., Zimmermann, R., Zechner, R., Teusink, B., Maassen, J. A., Havekes, L. M., and Romijn, J. A. (2003) *Endocrinology*. **144**, 3456-3462
49. Merglen, A., Theander, S., Rubi, B., Chaffard, G., Wollheim, C. B., and Maechler, P. (2004) *Endocrinology*. **145**, 667-678
50. Le, N. H., van der Wal A, van der Bent P, Lantinga-van Leeuwen, I., Breuning, M. H., van Dam H, de Heer E, and Peters, D. J. (2005) *J. Am. Soc. Nephrol.* **16**, 2724-2731
51. Pinkse, G. G., Steenvoorde, E., Hogendoorn, S., Noteborn, M., Terpstra, O. T., Bruijn, J. A., and de Heer E. (2004) *Diabetologia*. **47**, 55-61
52. Ouwens, D. M., Boer, C., Fodor, M., de, G. P., Heine, R. J., Maassen, J. A., and Diamant, M. (2005) *Diabetologia* **48**, 1229-1237